Preparation and evaluation of βcyclodextrin-based nanosponges loaded with Budesonide for pulmonary delivery

Preparation and Evaluation of β-Cyclodextrin-based Nanosponges loaded with Budesonide for Pulmonary Delivery

Yasmein Yaser Salem[a], Gjylije Hoti[b,c], Rana M.F. Sammour[a], Fabrizio Caldera[b], Claudio Cecone[b], Adrián Matencio[b], Aliasgar F. Shahiwala[a,*] Francesco Trotta[b,*]

[a]*Department of Pharmaceutics, Dubai Pharmacy College for Girls, Al Muhaisanah 1, Al Mizhar, 19099 Dubai, United Arab Emirates*

[b]*Department of Chemistry, University of Turin, Via P. Giuria 7, 10125 Turin, Italy*

[c] *Department of Drug Science and Technology, University of Turin, Via P. Giuria 9, 10125 Turin, Italy (Current Affiliation)*

[*]Corresponding authors: +971552563898 (Aliasgar F. Shahiwala); +39 0116707550 (Francesco Trotta). E-mail addresses: dr.asgar@dpc.edu (Aliasgar F. Shahiwala), francesco.trotta@unito.it (Francesco Trotta).

yasmein@dpc.edu (Yasmein Yaser Salem); gjylije.hoti@unito.it (Gjylije Hoti); rana@dpc.edu (Rana M.F. Sammour); fabrizio.caldera@unito.it (Fabrizio Caldera); claudio.cecone@unito.it (Claudio Cecone); adrian.matencioduran@unito.it (Adrián Matencio).

Abstract

Budesonide (BUD) is a glucocorticosteroid used to treat chronic obstructive pulmonary disease. Despite this, it is a hydrophobic compound with low bioavailability. To address these hurdles, non-toxic and biocompatible cyclodextrin-based nanosponges (βCD-NS) were attempted. BUD was loaded on five different βCD-NS at four different ratios. NS with 1,1'-carbonyldiimidazole (CDI) as a crosslinking agent, presented a higher encapsulation efficiency (~80%) of BUD at 1:3 BUD: βCD-NS ratio (BUD-βCD-NS). The optimized formulations were characterized by Fourier-transform infrared spectroscopy (FTIR), thermogravimetric analysis (TGA), water absorption capacity (WAC), scanning electron microscopy (SEM), X-ray powder diffraction studies (XRD), particle size, zeta potential, encapsulation efficiency, in vitro and in vivo release studies, acute toxicity study, solid-state characterization, and aerosol performance. In vitro-in vivo correlation and cytotoxicity of the formulations on alveolar cells in vitro were further determined. In vitro and in vivo studies showed almost complete drug release and drug absorption from the lungs in the initial 2 hours for pure BUD, which were sustained up to 12 hours from BUD loaded into nanosponges (BUD-βCD-NS). Acute toxicity studies and in vitro cytotoxicity studies on alveolar cells proved the safety of BUD-βCD-NS. Several parameters, including particle size, median mass aerodynamic diameter, % fine particle fraction, and % emitted dose, were evaluated for aerosol performance, suggesting the capability of BUD-βCD-NS to formulate as a dry powder inhaler (DPI) with a suitable diluent. To sum up, this research will offer new insights into the future advancement of βCD-NS as drug delivery systems for providing controlled release of therapeutic agents against pulmonary disease.

KEYWORDS: Pulmonary disease; Budesonide; Cyclodextrin nanosponges; In vitro and in vivo studies; Dry powder inhaler.

1.Introduction

Respiratory diseases, especially lung diseases, are recognized to cause almost 4 million deaths yearly, representing a major global health issue [1], [2]. Drug delivery systems (DDSs) are designed as engineered devices for the controlled release or targeted delivery of active components. The drug is usually encapsulated within a biocompatible shell, protecting against premature degradation due to physicochemical and biological factors. Drug carriers may contain different materials like lipids, metals, and natural or synthetic polymers. Improving bioavailability, prolonging circulation, controlling release kinetics, and reducing the risk of adverse effects of drugs are the main advantages of DDSs. The carriers in DDSs may deliver drugs in various ways, such as implantable, transdermal, parenteral, or pulmonary. Pulmonary DDSs remain the most popular in treating many respiratory diseases, such as asthma and chronic obstructive pulmonary disease. Compared with transdermal, oral, intravenous, ocular, or nasal administration, pulmonary drug delivery, as a non-invasive route for treating diseases, provides many advantages and therefore is preferred by patients [3]–[5]. Due to the physiology of lungs and their favorable properties, such as the large surface area (around 100 m^2, estimated to approximate the tennis court area) and excellent vascularization, pulmonary drug delivery displays a unique potential to deliver drugs systematically and locally [6]–[9]. The sustained-release formulations for pulmonary drug delivery have various advantages because of the reduced dosing frequency, side effects reduction, alveolar epithelium's high permeability, and patient compliance improvement [6], [10], [11]. Budesonide (BUD) is a potent corticosteroid with high glucocorticoid receptor affinity and prolonged tissue retention, inhibiting inflammatory symptoms such as vascular hyperpermeability and edema. BUD is a low molecular weight (430.53 Da), a non-halogenated second-generation synthetic glucocorticoid, structurally related to 16 α-hydroxyprednisolone with non-symmetric 16 alpha, 17 alpha-acetal, that is used for topical treatment of inflammatory bowel disease, rhinitis, asthma, treatment or reduction of the incidence of different lung diseases [7], [10]–[12]. BUD is one of the most widely used inhaled glucocorticoids with a high ratio of topical anti-inflammatory that reduces the number of inflammatory cells and mediators in the airways of asthma patients and minimizes the airway's hyper-responsiveness. The pharmacokinetic modeling presents the formation of the esters of BUD with large airways, lungs, and all tissues, thus sustaining local anti-inflammatory activity [11]. When administered orally, BUD undergoes a high first-pass elimination by the liver and approximately a complete absorption from the intestine, resulting in a low bioavailability of about 10% [10], [12]. BUD is characterized by an immediate absorption from the lung in both animals and humans and, therefore, is not expected to show a prolonged duration of action [13]. The hydrophobic nature, low oral bioavailability (6-11%), and short half-life (2-3 hours) of BUD are highlighted as major challenges to its clinical efficacy [11], [14]. To overcome this, several drug delivery systems were developed for BUD delivery.

Buhecha et al. encapsulated BUD in poly (lactic acid) (PLA) nanoparticles for pulmonary delivery using a double emulsification solvent diffusion (DESD) method. This investigation concluded that BUD-loaded PLA nanoparticles, due to the narrow size distribution and zeta potential with good BUD-loading efficiency, are suitable drug delivery systems for combination therapy of chronic obstructive pulmonary disease (COPD) and asthma [15].

Recently, Salem et al. proposed the inclusion of BUD with bilosomes as stable lipid vesicles. This study proved the potent effect of BUD-loaded bilosomal formulation on treating inflammation by decreasing the proinflammatory

cytokines TNF-α, and TGF-β contents and reducing protein kinase C (PKC) content in the lung [16].

Several studies presented cyclodextrins (CDs) as promising candidates in pulmonary delivery by increasing the solubility, bioavailability, and stability of water-insoluble and chemically unstable drugs [17]–[23]. Due to a unique typical toroidal cone shape with a lipophilic central cavity and a hydrophilic outer surface, CDs are well-known to play a significant role in drug delivery. CDs are low molecular weight (between 973 and 2163 Da) cyclic oligosaccharides that contain six (αCD), seven (βCD), eight (γCD), and a greater number of D-glucose units, joined through α-(1,4) glycosidic linkages [19], [24], [25].

However, CDs have several limitations, such as the inability to include certain hydrophilic compounds, high molecular weight drugs, and limited aqueous solubility (in particular, βCD). Therefore, to overcome these limitations, CDs can be chemically modified due to the availability of multiple reactive hydroxyl groups, and thus their application can be further expanded. Depending on the reaction and substituents, water-soluble and insoluble cyclodextrin-based polymers or cyclodextrin-based nanosponges (βCD-NS) are synthesized. βCD-NS are chemically crosslinked polymers that are obtained by reacting the cyclodextrin (CD) unit with a suitable crosslinking agent such as pyromellitic dianhydride (PMDA), 1, 1'-Carbonyldiimidazole (CDI), citric acid (CA), 1,4-Butanediol diglycidyl ether (BDE), etc [26], [27]. βCD-NS presents a remarkable encapsulation capacity. They improve the aqueous solubility of poorly water-soluble molecules, protect degradable substances, design innovative drug carriers, or obtain sustained delivery systems. The spherical shape and the small sizes of NS can affect the parenteral, pulmonary, and oral routes [28].

The studies regarding the pulmonary delivery of BUD-loaded CDs are minimal. Furthermore, investigating βCD-NS for pulmonary delivery is an innovative study. In this study, BUD was encapsulated into βCD-NS through three various methods. The formulations were characterized by FTIR Spectroscopy analysis, TGA analysis, water absorption capacity (WAC), scanning electron microscopy (SEM), X-ray powder diffraction studies (XRD), and by the measurement of the particle size, zeta potential, encapsulation efficiency, in vitro and in vivo release studies, acute toxicity study, solid-state characterization, and aerosol performance. In vitro/ in vivo correlation and cytotoxicity of the formulations on alveolar cells in vitro were further determined.

The advantages of pulmonary drug delivery and the outstanding attributes of nanosponges (NS) will contribute to an ideal drug delivery approach.

2. Experimental

2.1. Reagents

Dextrins such as β-Cyclodextrin (βCD; M_w=1134.98 g/mol) and KLEPTOSE® Linecaps (LC; M_w=~12000 g/mol), were kindly provided as a gift by Roquette (Lestrem, France). Dextrins were dried in the oven at 80 ^{0}C up to constant weight before their usage to remove any moisture content. Pyromellitic dianhydride (PMDA, 97%); Dimethylsulfoxide (DMSO, (≥99.90%); Triethylamine (Et_3N, ≥99.00%); Acetone (≥99.00% (GC)); 1, 1'-Carbonyldiimidazole (CDI, ≥97.00%); Sodium hypophosphite monohydrate (SHP, ≥99.00%); 1,4-Butanediol diglycidyl ether (BDE, technical grade, 60%); 1, 4-Diazabicyclo [2.2.2] octane (DABCO, ≥99.00%); N, N- Dimethylformamide (DMF, ≥99.80% (GC)); Sodium hydroxide (NaOH, pellets); Calcium hydride (CaH_2, 95.00%) were purchased from Sigma-Aldrich (Darmstadt, Germany). Budesonide (BUD, 97.00%) was purchased from ACROS Organics (Thermo Fisher Scientific, USA). The citric acid (CA, 99.90%) was purchased from VWR Chemicals BDH (Milano, Italy). Laboratory-grade Potassium chloride, Dibasic sodium phosphate, Potassium dihydrogen phosphate, Ethanol, and Dichloromethane were obtained

from SD Fine Chemicals Limited, Mumbai, India. DMF is treated with calcium hydride for anhydrification and filtered before use.

2.2. Study in Animals

An in vivo release study was performed on female rats weighing 190-200 g. The study was conducted following the Declaration of Helsinki and approved by the Institutional Review Board (or Ethics Committee) of Dubai Pharmacy College (REC/Mpharma/PPD/2021/03 dated 4th September 2021). The angle of repose, compressibility index, and Hausner ratio were determined as per United States Pharmacopeia and National Formulary (USP27-NF32).

2.3. Synthesis of βCyclodextrin-based nanosponges (βCD-based NS)

2.3.1. Synthesis of βCyclodextrin: Carbonyldiimidazole-based Nanosponge (βCD: CDI-based NS)

The synthesis of nanosponge (Figure 1) was carried out, following the procedure in the literature with some modifications [29]. 5.00 g of anhydrous βCD were dissolved in 30.00 mL of DMF in a round bottom flask, using a hotplate stirrer equipped with thermoregulation and heat-on block with the subsequent addition of 2.85 g of CDI as a crosslinking agent. The nanosponge was prepared with a stoichiometric ratio of 0.571 mole of CDI per mole of glucose unit. After a clear solution was observed, the temperature increased to 80 ^{0}C until the gel formed. Further, the formed gel was kept at 90 ^{0}C for approximately 5 hours to complete the reaction and obtain a solid product that was allowed to stand for 24 hours. The solidified mass was broken up and manually ground in a mortar. Then, it was repeatedly stirred with an excess of deionized water until a clear supernatant solution was obtained. The purification process was speeded up by a Buchner filtration system using filter paper (Whatman No. 1, Whatman, Maidstone, UK). The by-products were completely removed in Speed Extractor (BUCHI E-914), with acetone, for around 40 minutes. Finally, the βCD: CDI nanosponge (βCD: CDI-based NS) was air-dried, milled, and utilized for characterization as a white homogeneous powder with a yield of 67%.

2.3.2. Synthesis of β-Cyclodextrin: Pyromellitic Dianhydride-based Nanosponge (βCD: PMDA-based NS)

The synthesis of nanosponge (Figure 1) was performed by dissolving 4.89 g of anhydrous βCD in 20.00 mL DMSO in a round bottom flask following the procedure already mentioned in the existing literature [30]. Afterwards, a transparent uniform mixture was observed and 1.25 mL of Et_3N was used as a catalyst with the subsequent addition of 3.75 g PMDA as a crosslinking agent by applying the stoichiometric ratio 0.571 mole of PMDA per mole of glucose unit. The crosslinking reaction was exothermic and, therefore, was carried out under intense magnetic stirring at room temperature. The polymerization was completed within a few minutes, obtaining a solid that was allowed to stand for 24 hours. The same purification and recovery procedures, as previously described for βCD: CDI-based NS, were utilized to obtain a white powder as the product with a yield of >95%.

2.3.3. Synthesis of dextrin: Citric acid-based Nanosponge (Dextrin: CA-based NS)

The synthesis of nanosponge (Figure 1) was carried out by dissolving 4.40 g anhydrous βCD, or LC, in 15 mL of deionized water with the subsequent addition of 0.80 g SHP as a catalyst and 2.98 g CA as a crosslinking agent, following the procedure in the existing literature [31]. The reaction was carried out in the oven, under vacuum, at 140 ^{0}C for 1 hour and 100 ^{0}C for 15 hours. The nanosponge was prepared with a stoichiometric ratio of 0.571 mole of CA

per mole of glucose unit. The solidified mass was broken up and manually ground in a mortar. Then, it was repeatedly stirred with an excess of deionized water until a clear supernatant solution was obtained. The purification process was speeded up by the Buchner filtration system, using deionized water and acetone to remove the by-products. Finally, the synthesized product was air-dried, milled, and utilized for characterization as a homogeneous powder with a yield of ~ 60% (LC: CA-based NS and βCD: CA-based NS).

2.3.4. Synthesis of βCyclodextrin: 1,4-Butanediol diglycidyl ether-based nanosponge (BDE-based NS)

The synthesis of the nanosponge (Figure 1) was carried out with a procedure previously developed by our research group [32], with slight modifications. In a round-bottom flask, 7.50 g of anhydrous βCD was initially dissolved in 20.00 mL of 0.20 M NaOH aqueous solution. After a clear solution was observed, 0.37 g of DABCO was added under continuous stirring. After that, 4.85 mL of BDE was added, and the obtained transparent liquid was heated up to 90 °C using a hotplate stirrer equipped with thermoregulation and a heat-on block to maintain constant heating of the flask. The nanosponge was prepared with a stoichiometric ratio of 0.571 mole of BDE per mole of glucose unit. The reaction was then allowed to occur for 90 minutes, and a monolith block was obtained as the product. The synthesized product was recovered from the flask with a spatula and purified with deionized water to remove by-products. After purification, it was dried in an oven at 70 °C up to a constant weight and subsequently ground with a mortar to obtain a final powder with a yield of ~85%.

2.4. Budesonide loading into Nanosponge (BUD-NS)

The Budesonide (BUD) was loaded into the synthesized nanosponges (NS) following three different methods (Figure 2). The study was performed in a temperature-controlled room (21°C) under dark conditions. The formulation vessels were also covered during the experiment. Table 1 presents the preparation of various formulations.

Method A

According to the first loading method, the synthesized nanosponges (NS) (βCD: CDI-based NS; βCD: PMDA-based NS; Dextrin: CA-based NS; βCD: BDE -based NS) were placed in 5 mL Budesonide (BUD) ethanolic solution (2 mg/mL) in weight ratios (BUD: NS; 1:1; 1:2; 1:3; 1:4 w:w) (Figure 2 (a)). The dispersions (BUD: NS) were shaken for 24 hours at room temperature. The BUD-loaded NS were collected by centrifugation at 5,000 rpm for 4 minutes.

Method B

The second loading method (Figure 2 (b)) employed the immersion of the synthesized NS in 0.5 mL of deionized water and shaking for 24 hours. Afterward, 5 mL of Budesonide in ethanol solution (2 mg/mL) was added in weight ratios (BUD: NS; 1: 1; 1: 2; 1: 3; 1: 4; w:w). The dispersions (BUD: NS) were shaken for 24 hours at room temperature. The BUD-loaded NS were collected by centrifugation at 5,000 rpm for 4 minutes.

Method C

Further, the third loading method (Figure 2 (c)) was followed by the addition of NS in 5 mL of Budesonide dichloromethane solution (2 mg/mL) in weight ratios (BUD: NS; 1: 1; 1: 2; 1: 3; 1: 4 w:w). The dispersions (BUD: NS) were shaken for 24 hours at room temperature. The BUD-loaded NS were collected by centrifugation at 5,000 rpm for 4 minutes.

2.5. Physicochemical characterization

2.5.1. Particle Size, Polydispersity index, and Zeta potential

The particle size, polydispersity index (PDI), and zeta potential were determined by using the laser diffraction particle size analyzer (Litesizer 500, Anton Paar, Austria). A disposable cell filled with 1 mL of the blank (deionized water) and 10% w/v loaded aqueous NS formulation were used for particle size and PDI measurement. On the other hand, an omega cell was used to determine the zeta potential (ζ-potential). Three measurements were carried out, and their average was expressed as mean values ± SD.

2.5.2. FTIR Spectroscopy Analysis

The pure BUD, synthesized NS, and BUD-loaded NS were characterized through Fourier Transform Infrared Spectroscopy (FTIR) using a Perkin Elmer Spectrum Spotlight 100 FTIR spectrophotometer equipped with Spectrum software. The FTIR spectra were gained in the spectral range of 4000-650 cm^{-1}, at a spectral resolution of 4 cm^{-1}, and sample/background scan number of 8. FTIR spectra were obtained using a versatile Attenuated Total Reflectance mode (FTIR-ATR) sampling accessory with a diamond crystal plate. FTIR-ATR measurements were performed on dried samples.

2.5.3. Thermogravimetric Analysis (TGA)

The thermal stability of the pure BUD, blank βCD-NS, and BUD-βCD-NS was studied by thermogravimetric analysis (TGA). TGA was carried out using a TA Instrument Thermogravimetric Analyzer (TGA Q500) from 25 ^{0}C up to 700 ^{0}C, under nitrogen (N_2) flow, and with a heating ramp rate of 10 ^{0}C/min. The gas flows applied in the balance and furnace section were 40 mL/min and 60 mL/min. About 10 mg of the sample was weighed in an aluminum pan for analysis.

2.5.4. Water absorption capacity (WAC)

The kinetics of βCD-NS swelling is studied by following their increase in weight and volume when immersed in water. The swelling measurements are performed by immersing 100 mg of dry powder in deionized water (in 12 mL test tubes filled up to 10 mL) and blending them, in the beginning, using a Vortex Mixer. The test tubes are sealed and maintained at room temperature. After 2 hours, the mixtures are centrifuged to obtain a layer of water-bound material and free unabsorbed water. After removing the supernatant, the residual amount of free water is blotted off using tissue paper, and the weight is recorded. The water absorption capacity (%WAC) is calculated using the following Equation 1 [30]:

$$\mathrm{WAC}\ (\%) = \frac{m_t - m_o}{m_o} \times 100 \quad (1)$$

-where m_t is the weight of the swollen sample at time t, and m_o is the initial weight of the dry sample.

2.5.5. Morphological characterization of BUD-loaded NS

The morphology of BUD, blank NS, and BUD-loaded NS is studied using scanning electron microscopy (SEM). The imaging is conducted with a Zeiss EVO 50 (Oberkochen, Germany) using secondary electrons and 10 kV accelerating voltage. The samples are placed on the aluminum stub with the help of a bio-adhesive carbon tape. Before SEM analysis, the polymers were coated with 12 nm of gold using a Desktop Sputter Coater model DSR1 provided by Vac Coat Ltd. (London, United Kingdom. NW11 8ED) for 40 seconds, under vacuum, at 45 mA.

2.5.6 X-ray powder diffraction studies (XRD)

The XRD spectra of BUD, blank NS, and BUD-loaded NS were recorded by a Malvern Panalytical X'Pert diffractometer using Cu Kal as a source of radiation. Data was collected over an angular range from 5 to 45 ^{0}2 theta at a step size of 0.017 ^{0}2 theta and a time per step of 100.33 s.

2.6. *Determination of Encapsulation Efficiency*

The dispersions (BUD: NS) were centrifuged at 5,000 rpm for 5 minutes, and the supernatant, containing free BUD, was collected. The drug content was determined by a UV-visible spectrophotometer (UV-1700, Pharma Spec, Shimadzu, Japan). The spectroscopic method was developed using 1:1 (v:v) water: ethanol mixture and a linear relationship was observed between 0-40 µg/mL of BUD with correlation coefficient value $R^2 > 0.999$ at λ_{max} 245.7 nm. The amount of unentrapped drug was calculated by referring to the BUD calibration curve. The encapsulation efficiency (EE%) was defined as the mass of encapsulated BUD (m_{en}) over its total mass ($m_{total\ drug}$) during the loading step, as presented in Equation 2 [31]:

$$\text{Encapsulation Efficiency (EE\%)} = \frac{m_{(en)}}{m_{(\text{total drug})}} \times 100 \quad (2)$$

The loading capacity (LC%) was defined as the mass of encapsulated BUD (m_{en}), divided by the total mass of nanosponge (NS) ($m_{total\ NS}$), as presented in Equation 3:

$$\text{Loading Capacity (LC\%)} = \frac{m_{(en)}}{m_{(\text{total NS})}} \times 100 \quad (3)$$

2.7. In vitro release study

In vitro release of BUD from the nanosponges was studied. In this procedure, 10 mg of BUD-βCD-NS was dispersed in 10 mL of simulated lung fluid (SLF) and kept at 37±0.5 °C with constant agitation (100 rpm) on a shaking machine. Phosphate-buffered saline (PBS) was the media used as SLF. At selected time intervals (0.5, 2, 4, and 6 hours), the aliquots (0.2 mL) were withdrawn and diluted to 10 mL with 1:1 (*v:v*) water: ethanol solution. The aliquots (0.2 mL) were replaced with an equivalent volume of fresh media. The amount of released drug was assessed with a UV-visible spectrophotometer at λ_{max} 245.7 nm.

2.8. In vivo release study

An in vivo release study was performed on female rats with a weight range of 190-200 g. Two groups of rats were allowed to acclimatize to the laboratory conditions for ten days before experimenting. Each group consisted of 6 rats. Rats were anesthetized using a combination of xylazine (100 mg/mL) and ketamine (100 mg/mL). Once anesthetized, a skin incision of 3 cm was made in front of the rat's throat (Figure 3 (a)).

Further, tissue adjacent to the trachea was removed, and an incision in the trachea was made (Figure 3 (b)). Then, the tube was inserted and fixed with a thread (Figure 3 (c)). The rats were gently administered (a dose equivalent to 0.2 mg BUD per 100 g rat body weight) through the inserted tube using a needle that was calculated according to their weight and dispersed in minimum volume (0.1 mL) of phosphate-buffered saline (PBS), pH 7.4 at 37 ^{0}C. The samples from the lungs were collected at different time intervals (0.5, 2, 4, 6, and 12 hours) using the lung lavage technique [33]. Lung lavage volume collected at zero time was considered 100% of the remaining drug. PBS was flushed into the lungs and withdrawn back. This was repeated thrice with 2 mL of fresh buffer each time to ensure the complete withdrawal of the remaining BUD from the lungs. Collected samples were extracted with dichloromethane solvent. The solvent was then evaporated, and the BUD was further dissolved in ethanol:water (50:50) to be spectrophotometrically analyzed. Conclusively, the percentage (%) of the remaining BUD in the lungs was calculated.

2.9. Acute toxicity study

For lethal dose 50% (LD50) determination, rats were divided into two groups, six in each group. The rats were fasted overnight and weighed preceding dosing with the respective formulation. A 15 mg/kg drug suspension and BUD-βCD-NS formulation containing an equivalent amount of drug were administered by an intratracheal route. The animals were observed for any signs of mortality. If the animals survived, a higher dose was administered, and the dose when two or more rats of the same group died was considered the LD50 value of the respective formulation. The dose intensification was planned in the order of 15, 30, and 40 mg/kg.

2.10. Solid state characterization and aerosol performance

The powder performance of the BUD-βCD-NS was evaluated using the Anderson Cascade Impactor. The eight-stage Anderson cascade impactor with a pre-separator was used to evaluate in vitro pulmonary deposition of BUD-βCD-NS powder at a 60 L/min flow rate. Briefly, the collection plate was placed below each filter, which was lodged within an airtight stage arranged successively on a level setting. A size '3' hard gelatin capsule was filled with 100 mg of formulation and aerosolized using an inhalator. Later, the air was pumped at a rate of 60 L/min through the stages using a vacuum pump. For the next 4 seconds, the powder was allowed to distribute among stages, after which airflow ceased. Three capsules were actuated for the impaction of each formulation, with each capsule for 4 seconds. The drug content deposited on different parts such as pre-separators, individual impaction plates, filters, powder sticking in capsules, and inhaler devices were then rinsed using methanol. Percentage emitted dose, fine particle fraction, mass median aerodynamic diameter, and geometric standard deviation were calculated from deposition data according to USP27-NF32.

2.11. In-vitro and in-vivo correlation (IVIVC)

Level A IVIVC between % in vitro drug release and % in vivo drug absorbed was investigated using linear – non-linear regression to determine the highest correlation (R^2).

2.12. Determination of cytotoxicity of the formulations on alveolar cells in vitro

To determine the safety of the formulation, a diploid human cell line composed of fibroblasts derived from lung tissue WI-38 was used in this study. This study was outsourced at Cairo University, Egypt and a detailed method of cytotoxicity is given in the supplementary data. The cells were cultured in Eagle's Minimum Essential Medium with 10% FBS and 1% penicillin/streptomycin at 37 °C with 95% humidity and 5% CO_2. A 96-well tissue culture plate was inoculated with 1 X 10^5 cells/ml (100 µl /well) and incubated at 37 °C for 24 hours to develop a complete monolayer sheet. The growth medium was decanted from 96-well microtiter plates after a confluent sheet of cells was formed, and the cell monolayer was washed twice with wash media. Two-fold dilutions of the tested sample were made in Roswell Park Memorial Institute (RPMI) 1640 medium with 2% serum (maintenance medium). A 0.1 mL of each dilution was tested in triplicate in different wells, leaving three wells as control, receiving only maintenance medium. The absorbance at 560 nm was measured with a reference wavelength of 620 nm using a microplate ELISA reader. After being exposed to the chemical for 24 hours, cell viability was calculated as a % of control. IC50 is the concentration of a formulation that inhibits 50 % of cell development and was determined using dose-response curve analysis through Graph Pad InStat version 3.00 for Windows 95, GraphPad Software Inc., San Diego California USA.

2.13. Statistical analysis

All experiments were performed in triplicate, and the data are expressed as mean values ± standard deviation (SD). A statistically significant change was considered at $p < 0.05$.

3. Results and discussion

3.1. Synthesis of βCyclodextrin-based nanosponges (βCD-NS)

The polymerization reactions led to a successful synthesis of dextrin-based NS (Figure 1). 1, 1'-Carbonyldiimidazole (CDI), pyromellitic dianhydride (PMDA), citric acid (CA), and 1,4-butanediol diglycidyl ether (BDE) were utilized as suitable crosslinking agents to react with dextrin unit. βCD-NS using CDI as a crosslinking agent presents short crosslinking bridges and good stability to slightly alkaline and acidic solutions. In contrast, βCD-NS which are synthesized from PMDA and CA undergo hydrolysis in aqueous media more than those with CDI. Further, βCD-NS synthesized with BDE are characterized by a high chemical resistance, yielding a stable covalent ether linkage [34]. The βCD-NS are synthesized by the reaction of the hydroxyl groups in the βCD structure with suitable crosslinking agents via nucleophilic attack at certain conditions (as it is detailed in Figure 1). The synthesized polymers are characterized by a three-dimensional network with different types of cavities, which will be beneficial for encapsulating either hydrophilic or lipophilic drugs and improving their solubility and bioavailability [35]. The resulting crosslinked products are further characterized to understand the interaction between BUD and NS. Furthermore, it is the first time βCD-NS were used to encapsulate BUD for pulmonary application.

3.2. Loading of BUD into βCD-NS

Initially, a suitable organic solvent had to be selected to dissolve BUD. In the first trial, ethanol was used during the loading procedure, and unreliable data on EE% were yielded. BUD was not incorporated into the βCD-NS, and a two-phase sediment was observed, indicating an unentrapped and undissolved BUD. For this reason, hydration of NS with 5 mL deionized water for 24 hours was performed before using the NS for loading. The results were recurrently unreliable, and therefore, BUD loading was carried out in a dichloromethane solution on a shaking machine for 24 hours (Figure 2).

3.3. Encapsulation efficiency (EE%)

Three loading methods were evaluated throughout the experiment, as shown in Table 2. Methods A and B produced unreliable results with a low EE%. However, method C resulted in a significantly high EE%. Moreover, βCD: CDI-NS showed an EE% of ~80%, where maximum drug loading was obtained in a weight ratio of 1:3 (BUD:βCD-NS). Based on these results, the F3 (BUD-βCD-NS), showing the highest EE%, was selected for further assessments.

3.4. Physicochemical characterization

The capacity of synthesized NS to absorb water, as a function of the presence of functional groups in the polymer matrix (Figure 1), was determined [30]. The ability to absorb water is considered an essential peculiarity of the crosslinked polymers influencing drug release rates. The release of a drug encapsulated into the polymer matrix is complex. The water absorption and the diffusion rate of the drug through the swollen polymer impact the total drug release [35]–[37]. Table 3 presents a lower swelling capacity of βCD:CDI NS than βCD:PMDA, βCD:CA, LC:CA, and βCD:BDE. This confirms what is already observed from the literature that the βCD-NS synthesized using CDI (carbonate NS) presents a reduced swelling ability than the ones using PMDA/ CA (ester NS) and BDE (ether NS) [34]. Although βCD:CDI NS absorbs water less than the other NS, it presented better drug loading and release behavior, maybe because of its high chemical resistance. The capacity of NS to absorb water will help the BUD delivery for pulmonary application since it is soluble in organic solvents and not in the water, thus totally avoiding the risk related to the direct use of organic solvents. Administering free drugs only soluble in an organic solvent is incompatible with pulmonary administration. Thus, βCD-NS can be considered a green incorporation strategy to improve the therapeutic efficiency of BUD for pulmonary delivery.

The results in Table 4 display a significant increase in particle size between blank and BUD-βCD-NS using a wet dispersed method, thus confirming the loading of BUD into NS. PDI values are within the accepted value of < 30% homogenous distribution.

To attain optimum clinical outcomes, the formulations of encapsulated therapeutic molecules with a narrow and constant size distribution are required [38]. The clinical effectiveness of a drug is influenced by the deposition of an aerosol in the lung that is dependent on particle size [4]. The particles <5 μm are considered to have the most significant potential for deposition in the lungs. The fine-particle fraction (FPF) is the proportion of the particles <5 μm within an aerosol that will be further discussed. Moreover, the particles 0.1-1 μm diffuse by Brownian motion and deposit when they collide with the airway wall [39]. The zeta potential of 5.2 mV (blank βCD-NS) was changed to a negative zeta potential of -2.6 mV (F3). This relatively fast change of zeta potential indicates the slight influence of BUD on the

physicochemical properties of blank βCD:CDI NS [40], [41].

FTIR-ATR spectra of BUD, βCD, CDI, blank βCD-NS, and BUD-βCD-NS are presented in Figure 4. The prominent absorption peaks of the NS appear at 2930, 1740, and 1022-1000 $cm^{-1,}$ and they can be assigned to the stretching vibration of C-H, C=O, and C-O bonds, respectively. Furthermore, broadband related to the stretching vibration of O-H bonds is visible in the 3650-3000 cm^{-1} range. The synthesized polymers and prepared formulations present comparable spectra with similar bands at characteristic wavenumbers and similar relative intensities, which does not provide the interaction of BUD with NS. Moreover, the typical peak at 1740 cm^{-1} corresponding to the C=O stretching vibration of the crosslinking group is evidence of the NS formation. This carbonyl peak at 1740 cm^{-1} does not appear in the FTIR spectrum of βCD, confirming the crosslinking process between βCD and CDI. Since the development of pulmonary delivery is highly dependent on the knowledge of the polymer-drug interactions, other investigation methods were highly required.

The thermal stability of the products in this study was analyzed by the TGA. The thermograms of pure BUD, βCD, CDI, blank NS, and BUD-βCD-NS are presented in Figure 5. Budesonide degrades at a temperature above 250 ^{0}C. The blank NS undergoes an initial 10% weight loss before 150 °C due to the release of moisture and starts the degradation above 200 ^{0}C. βCD does not present any considerable presence of moisture since it is always kept anhydrous in the oven before its usage (Subsection 2.1.) but presents a degradation temperature above 270 ^{0}C. The differences in the thermograms of the TGA curves of βCD-NS from the βCD are due to changes in chemical structure [42], [43]. Furthermore, the TGA of BUD-βCD-NS presents a similar maximum degradation behavior to blank NS. The presented results can only indicate the good thermal stability of the prepared formulations.

3.5. Morphological characterization of BUD-loaded NS

The scanning electron microscope (SEM) was used to determine the surface morphology of the BUD, βCD-NS+ BUD physical mixture, and BUD-βCD-NS as presented in Figures 6 a), b), and c). SEM images at 5000 magnifications confirmed the heterogeneous polymer surface. Figure 6 shows a highly irregular surface of the samples, and no significant differences were observed regarding the size and morphology of BUD and BUD-βCD-NS. SEM image (Figure 6 b)) of the physical mixture shows the deposition of free drug particles on the NS surface, which was absent in the SEM of the optimized formulation, confirming the entrapment of the drug inside the NS porous structure.

3.6. XRD-diffraction analysis

XRD diffraction diagrams of BUD-βCD-NS, βCD-NS+ BUD physical mixture, and BUD are shown in Figures 7 a), b), and c). For preparing the physical mixture, the same quantity of BUD (Subsection 2.4, method C of loading) was mixed with the βCD-NS powder in a mortar for a certain time at room temperature. The absence of high-intensity peaks in the X-ray diffractogram of BUD-βCD-NS (Figure 7 a)) can be related to the amorphous nature of βCD-NS that contains no sharp crystalline peaks. Whereas, the crystalline nature of BUD (Figure 7 c)) is presented with many intense peaks in the X-ray diffractogram between 10^0 theta to 25^0 theta (Figure 7 c)). However, in the case of βCD-NS+ BUD physical mixture the characteristic peaks of BUD were noticeable with lesser intensity, suggesting no change in the

property of BUD that remains in the crystalline form (Figure 7 b). The XRD diffraction results confirm the formulation's amorphization process, which is evident in the inclusion complex formation [44].

3.7. In vitro drug release

The release pattern carried out for 12 hours showed a more sustained release for F3 than the pure BUD (as shown in Table 5 and Figure 8). The pure BUD (~70%) was released in 30 minutes. In contrast, the F3 presented 65% BUD release within 6 hours, proving the sustained release of the selected F3. The rapid release of free BUD can be related to its rapid diffusion in PBS. In contrast, the slow release of BUD encapsulated into the NS can be explained by the diffusion of BUD from a crosslinked polymeric network of NS. The sustained release expresses the longer retention of BUD in the lung, which diminishes its exhalation and systemic toxicity. This is essential to achieve optimum therapeutic efficacy of BUD and it is obtainable in the market as a conventional dry powder inhaler (DPI) and presents only 30% of deposition in the lung [14]. Although BUD was successfully encapsulated in cyclodextrins (CDs) and consequently, its solubility and bioavailability were enhanced [22], βCD-NS are well-known to overcome the limitations of native CDs [26,46,47,49].

3.8. In vivo drug release

The results of the *in-vivo* study of BUD-βCD-NS and pure BUD are presented in Table 6 and Figure 9. The pure BUD (~50%) was cleared from the lungs in 30 minutes and 94% within the first 2 hours of administration. At the same time, the BUD-βCD-NS presented 41% BUD remaining in the lungs after 6 hours. The percentage of BUD remaining from F3 conveyed sustained release in comparison to pure BUD. Therefore, it is indicated that a formulation of βCD-NS can sustain the release and improve the solubility of BUD.

3.9. *Acute Toxicity Studies*

LD50 was determined by observing signs of morbidity and mortality in rats after administration of respective formulations. The dose escalation was performed in the 15, 30, and 40 mg/kg sequence. No animal died at the end of the study, indicating the safe administration of BUD-βCD-NS. Since no study has been reported on the pulmonary administration of NS, it can be predicted that the ester bonds in βCD: CDI NS can easily be hydrolyzed by enzymes in the alveolar fluid [48]. CDs are readily absorbed from the lung, and the absorption rate varies between different CDs, with one study reporting Hydroxypropyl- β -cyclodextrin (HP-βCD) as the best candidate as a drug carrier for sustained pulmonary delivery [21]. In general, CDs are proven to be safe for pulmonary application [19], [49]–[51]. Natural CDs (α-, β- and γ-CD) were safe in human bronchial adenocarcinoma-derived Calu-3 cells [52].

Similarly, a synthetic derivative of βCD, sulfobutylether-β-cyclodextrin (SBE-βCD), was found to be safe in human lung adenocarcinoma cell line (A549) when formulated as a DPI containing fisetin-SBE-βCD complex to deliver high amounts of fisetin to the deep lung region for therapeutic purposes [20]. Polymeric βCD (crosslinked βCD with epichlorohydrin) was also well tolerated in mice when repeatedly administered to the lungs in high doses [53]. All these studies suggest the NS used in this study is likely well tolerated for repeated pulmonary applications. Shende et al. (2012), in an already published acute toxicity study, presented the oral administration of βCD: PMDA NS in rats at the dose of 2000 mg/kg. No animals died and no signs of toxicity up to 14 days were observed. This study has proven the non-toxic βCD NS in rats to an oral dose of 2000 mg/kg of body weight [54]. As the toxicological evaluation is a

significant step to determine the safety of drugs and to select safe doses for their usage in humans and animals, Shende et al. (2015) designed another study to evaluate the toxicity of different NS formulations with crosslinking agents such as 1, 1'-carbonyldiimidazole (CDI), pyromellitic dianhydride (PMDA), and hexamethylene diisocyanate (HMDI). During the acute toxicity study, after a single oral administration of NS samples at 300 and 2000 mg/kg dose levels, animals in all treated groups showed no lethal effects or mortality. In addition, administration of test NS formulation, through the repeated dose toxicity study, for 28 days did not display any adverse symptoms of mortality and toxicity. All NS formulations presented no hepatic or renal toxicity. The observations in this study support the safety compounds in rats since the histopathological examination of essential organs such as the kidney, liver, stomach, and intestine displayed no damage. Therefore, this study provided a completed report on toxicity data of the βCD-NS after oral administration, considering this polymeric system as a new platform for drug delivery with the potential of ameliorating oral therapeutic formulations [55]. However, further acute and chronic studies are required before culminating in the safety of BUD-βCD-NS formulation for pulmonary delivery.

3.10.*Solid state characterization and Aerosol performance*

As it is shown in Table 7, the low angle of repose, compressibility index, and Hausner ratio suggest the excellent flowing property of BUD-βCD-NS.

A cascade impactor was used to evaluate aerosol performance, maintaining the vacuum at 60 L/min. Several parameters, including formulation delivered dose, fine particle dose (FPD), median mass aerodynamic diameter (MMAD), % fine particle fraction (%FPF), % emitted dose (%ED), and dispersibility containing different cryoprotectants in selected ratios, were derived as mentioned in USP27-NF32. Deviation in the previously mentioned properties presented a significant difference in-vivo performance of the formulations. MMAD values of the formulation govern the distribution of powder throughout the lungs. It is observed that MMAD of more than five leads to deposition of formulation around the trachea and upper portion of the lungs, while MMAD lower than 1 causes systemic absorption of the formulation after reaching the alveoli. BUD-βCD-NS showed an MMAD value of 4.17±0.30 and a geometric standard deviation (GSD) of 2.10±0.20, which justifies the deeper penetration capability of the formulation. These results correspond to the particle size determined by the SEM.

Additionally, it possessed an FPF of 45.14±3.60% with a % emitted dose of 92.40±0.84. The higher values of % FPF indicated its deposition towards the lower stages of the impactor. Additionally, the non-hygroscopic nature of BUD ensured around 92% of dose emission, which circumvented the problem of dose variables. The results proved the capability of BUD-βCD-NS to formulate a dry powder inhaler (DPI) with a suitable diluent.

3.11.IVIVC

This work further seeks to establish a point-to-point (level A) relationship between the in vitro drug release and the in vivo absorption rate of BUD from the NS. Linear correlations ($R^2 > 0.9743$) between the % drug released in vitro and the % drug absorbed in vivo fraction were successfully established for the BUD-βCD-NS (Figure 10) and considered an excellent relationship [56].

3.12. Determination of cytotoxicity of the formulations on alveolar cells in vitro

The optimized BUD-βCD-NS formulation's functional assay (MTT) (viability/cytotoxicity) was performed using the WI38 cell line. The detailed results are provided in the Supplementary file (S1). The IC50 of BUD-βCD-NS formulation was > 500 µg/mL (560.1 ± 3.34) (Table S1). BUD-βCD-NS formulation does not induce any abnormalities in cell morphology, intracellular trafficking, and cell cycle up to concentrations of 500 µg mL^{-1}, which is considered safe for application [57].

4.Conclusions

BUD was successfully loaded into βCD-NS by the third loading method (method C; carried out in dichloromethane solution). The highest BUD encapsulation efficiency (81 ± 5.0%) was observed for the BUD loaded into βCD: CDI-NS formulation. In vitro and in vivo studies displayed almost complete drug release and drug absorption from the lungs in the initial 2 hours for pure BUD, which were sustained up to 12 hours from BUD loaded into nanosponges (BUD-βCD-NS). Acute toxicity studies and in vitro cytotoxicity studies on alveolar cells proved the safety of BUD-βCD-NS. Several parameters, including particle size, median mass aerodynamic diameter, % fine particle fraction, and % emitted dose, were evaluated for aerosol performance, suggesting the capability of BUD-βCD-NS to formulate as a dry powder inhaler (DPI) with a suitable diluent.

To sum up, this research presents the great potential of using the βCD-NS to deliver therapeutics via the pulmonary route. Thus, it will encourage their outstanding application as common treatment. This study was intended to formulate a BUD-βCD-NS dry powder inhaler. The development of inhaled therapy will lead to existing delivery or new drugs using novel delivery systems.

Acknowledgments

Authors acknowledge support from the Dubai Pharmacy College for Girls and Project CH4.0 under the MUR program "Dipartimenti di Eccellenza 2023-2027" (CUP: D13C22003520001).

Conflicts of interest

The authors declare no conflicts of interest.

References

[1] V. Forest and J. Pourchez, "Nano-delivery to the lung - by inhalation or other routes and why nano when micro is largely sufficient?," *Adv. Drug Deliv. Rev.*, vol. 183, pp. 1–54, 2022.

[2] L. Zhang *et al.*, "Sustained therapeutic efficacy of budesonide-loaded chitosan swellable microparticles after lung delivery: Influence of in vitro release, treatment interval and dose," *J. Control. Release*, vol. 283, pp. 163–174, 2018.

[3] S. Magramane, Z. Pápay, B. Turbucz, and I. Antal, "Formulation and Characterization of Pulmonary Drug Delivery Systems," *Acta Pharm. Hung.*, vol. 89, no. 2, pp. 63–83, 2019.

[4] N. R. Labiris and M. B. Dolovich, "Pulmonary drug delivery. Part I: Physiological factors affecting therapeutic effectiveness of aerosolized medications," *Br. J. Clin. Pharmacol.*, vol. 56, no. 6, pp. 588–599, 2003.

[5] D. La Zara *et al.*, "Controlled Pulmonary Delivery of Carrier-Free Budesonide Dry Powder by Atomic Layer Deposition," *ACS Nano*, vol. 15, no. 4, pp. 6684–6698, 2021.

[6] K. Knap, K. Kwiecień, K. Reczyńska-Kolman, and E. Pamuła, "Inhalable microparticles as drug delivery systems to the lungs in a dry powder formulations," *Regen. Biomater.*, vol. 10, pp. 1–31, 2023.

[7] C. García-Mouton *et al.*, "Beyond the Interface: Improved Pulmonary Surfactant-Assisted Drug Delivery through Surface-Associated Structures," *Pharmaceutics*, vol. 15, no. 256, pp. 1–18, 2023.

[8] D. A. Edwards, A. Ben-Jebria, and R. Langer, "Recent advances in pulmonary drug delivery using large, porous inhaled particles," *Invit. Rev.*, pp. 379–385, 2023.

[9] S. P. Newman, "Drug delivery to the lungs: challenges and opportunities," *Ther. Deliv.*, vol. 8, no. 8, pp. 647–661, 2017.

[10] W. Hempfling, F. Grunhage, K. Dilger, C. Reichel, U. Beuers, and T. Sauerbruch, "Pharmacokinetics and Pharmacodynamic Action of Budesonide in Early- and Late-Stage Primary Biliary Cirrhosis," *Hepatology*, vol. 38, no. 1, pp. 196–202, 2003.

[11] S. R. Naikwade, A. N. Bajaj, P. Gurav, M. M. Gatne, and P. Singh Soni, "Development of Budesonide Microparticles Using Spray-Drying Technology for Pulmonary Administration: Design, Characterization, In Vitro Evaluation, and In vivo efficacy study," *AAPS PharmSciTech*, vol. 10, no. 3, pp. 993–1012, 2009.

[12] L. Del Vecchio, C. Rimoldi, and C. Pozzi, "Nefecon (targeted-release formulation-budesonide) for the treatment of IgA nephropathy," *Futur. Rare Dis.*, vol. 1, no. 4, p. 14, 2021.

[13] M. Jendbro, C.-J. Johansson, P. Strandberg, H. Falk-Nilsson, and S. Edsbäcker, "Pharmacokinetics of Budesonide and its major Ester Metabolite after Inhalation and Intravenous Administration of Budesonide in the Rat," *Drug Metab. Dispos.*, vol. 29, no. 5, pp. 769–776, 2001.

[14] A. J. Mali, A. P. Pawar, and R. N. Purohit, " Development of Budesonide Loaded Biopolymer Based Dry Powder Inhaler: Optimization, In Vitro Deposition, and Cytotoxicity Study ," *J. Pharm.*, vol. 2014, pp. 1–12, 2014.

[15] M. D. Buhecha, A. B. Lansley, S. Somavarapu, and A. S. Pannala, "Development and characterization of PLA nanoparticles for pulmonary drug delivery: Co-encapsulation of theophylline and budesonide, a hydrophilic and lipophilic drug," *J. Drug Deliv. Sci. Technol.*, vol. 53, pp. 1–13, 2019.

566[16] H. F. Salem, G. A. Moubarak, A. A. Ali, A. A. A. Salama, and A. H. Salama, “Budesonide-Loaded Bilosomes
567 as a Targeted Delivery Therapeutic Approach Against Acute Lung Injury in Rats,” *J. Pharm. Sci.*, vol. 112, pp.
568 760–770, 2023.
569[17] Á. Haimhoffer *et al.*, “Cyclodextrins in Drug Delivery Systems and Their Effects on Biological Barriers,” *Sci.*
570 *Pharm.*, vol. 87, no. 33, pp. 1–21, 2019.
571[18] S. V. Kurkov and T. Loftsson, “Cyclodextrins,” *Int. J. Pharm.*, vol. 453, no. 1, pp. 167–180, 2013.
572[19] T. Loftsson, P. Jarho, M. Másson, and T. Järvinen, “Cyclodextrins in drug delivery,” *Expert Opin. Drug Deliv.*,
573 vol. 2, no. 2, pp. 335–351, 2005.
574[20] N. Mohtar, K. M. G. Taylor, K. Sheikh, and S. Somavarapu, “Design and development of dry powder
575 sulfobutylether-β-cyclodextrin complex for pulmonary delivery of fisetin,” *Eur. J. Pharm. Biopharm.*, vol. 113,
576 pp. 1–10, 2017.
577[21] M. Guan *et al.*, “Characterization, in Vitro and in Vivo Evaluation of Naringenin-Hydroxypropyl-ß-
578 Cyclodextrin Inclusion for Pulmonary Delivery,” *Molecules*, vol. 25, no. 554, pp. 1–15, 2020.
579[22] G. Michailidou, G. Z. Papageorgiou, and D. N. Bikiaris, “β-Cyclodextrin Inclusion Complexes of Budesonide
580 with Enhanced Bioavailability for COPD Treatment,” *Appl. Sci.*, vol. 11, no. 12085, pp. 1–15, 2021.
581[23] T. Kinnarinen, P. Jarho, K. Järvinen, and T. Järvinen, “Pulmonary deposition of a budesonide / γ-cyclodextrin
582 complex in vitro,” *J. Control. Release*, vol. 90, pp. 197–205, 2003.
583[24] M. E. Brewster and T. Loftsson, “Cyclodextrins as pharmaceutical solubilizers,” *Adv. Drug Deliv. Rev.*, vol. 59,
584 pp. 645–666, 2007.
585[25] E. M. M. Del Valle, “Cyclodextrins and their uses: A review,” *Process Biochem.*, vol. 39, no. 9, pp. 1033–1046,
586 2004.
587[26] F. Trotta, “Cyclodextrin Nanosponges and their Applications,” in *Cyclodextrins in Pharmaceutics, Cosmetics,*
588 *and Biomedicine*, Hoboken, NJ, USA: John Wiley & Sons, Inc., 2011, pp. 323–342.
589[27] T. Loftsson and M. E. Brewster, “Pharmaceutical Applications of Cyclodextrins . 1 . Drug Solubilization and
590 Stabilization,” *J. Pharm. Sci.*, vol. 85, no. 10, pp. 1017–1025, 1996.
591[28] F. Trotta and R. Cavalli, “Characterization and applications of new hyper-cross-linked cyclodextrins,” *Compos.*
592 *Interfaces*, vol. 16, no. 1, pp. 39–48, Feb. 2009.
593[29] M. R. P. Rao, J. Chaudhari, F. Trotta, and F. Caldera, “Investigation of Cyclodextrin-Based Nanosponges for
594 Solubility and Bioavailability Enhancement of Rilpivirine,” *AAPS PharmSciTech*, vol. 19, no. 5, pp. 2358–
595 2369, 2018.
596[30] G. Hoti *et al.*, “Effect of the Cross-linking Density on the Swelling and Rheological Behavior of Ester-Bridged
597 β-Cyclodextrin Nanosponges,” *Materials (Basel).*, vol. 14, no. 3, pp. 1–20, 2021.
598[31] G. Hoti *et al.*, “A Comparison between the Molecularly Imprinted and Non-Molecularly Imprinted
599 Cyclodextrin-based Nanosponges for the Transdermal Delivery of Melatonin,” *Polymers (Basel).*, vol. 15, no.
600 1543, pp. 1–27, 2023.
601[32] C. Cecone, G. Costamagna, M. Ginepro, and F. Trotta, “One-step sustainable synthesis of cationic high-
602 swelling polymers obtained from starch-derived maltodextrins,” *RSC Adv.*, vol. 11, pp. 7653–7662, 2021.
603[33] J.-A. Song *et al.*, “Standardization of Bronchoalveolar Lavage Method Based on Suction Frequency Number

and Lavage Fraction Number Using Rats," *Toxicol. Res.*, vol. 26, no. 3, pp. 203–208, 2010.

[34] F. Caldera, M. Tannous, R. Cavalli, M. Zanetti, and F. Trotta, "Evolution of Cyclodextrin Nanosponges," *Int. J. Pharm.*, vol. 531, no. 2, pp. 470–479, 2017.

[35] B. Rossi *et al.*, "Probing the molecular connectivity of water confined in polymer hydrogels," *J. Chem. Phys.*, vol. 142, no. 1, p. 14, 2015.

[36] F. M. Carbinatto, A. D. de Castro, R. C. Evangelista, and B. S. F. Cury, "Insights into the swelling process and drug release mechanisms from cross-linked pectin/high amylose starch matrices," *Asian J. Pharm. Sci.*, vol. 9, no. 1, pp. 27–34, 2014.

[37] W. L. S.C., P. W. S. Heng, and L. F. Wong, "Relationship between swelling and drug release in a hydrophilic matrix," *Drug Dev. Ind. Pharm.*, vol. 19, no. 10, pp. 1201–1210, 1993.

[38] M. Danaei *et al.*, "Impact of Particle Size and Polydispersity Index on the Clinical Applications of Lipidic Nanocarrier Systems," *Pharmaceutics*, vol. 10, no. 57, pp. 1–17, 2018.

[39] B. L. Laube *et al.*, "What the pulmonary specialist should know about the new inhalation therapies," *Eur. Respir. J.*, vol. 37, no. 6, pp. 1308–1331, 2011.

[40] D. Thiyagarajan *et al.*, "Spray-dried lactose-leucine microparticles for pulmonary delivery of antimycobacterial nanopharmaceuticals," *Drug Deliv. Transl. Res.*, vol. 11, pp. 1766–1778, 2021.

[41] F. Prüfert, F. Fischer, C. Leichner, S. Zaichik, and A. Bernkop-Schnürch, "Development and In Vitro Evaluation of Stearic Acid Phosphotyrosine Amide as New Excipient for Zeta Potential Changing Self-Emulsifying Drug Delivery Systems," *Pharm. Res.*, vol. 37, no. 4, p. 9, 2020.

[42] I. Asela, O. Donoso-Gonzalez, N. Yutronic, and R. Sierpe, "β -Cyclodextrin-Based Nanosponges Functionalized with Drugs and Gold Nanoparticles," *Pharmaceutics*, vol. 13, no. 513, pp. 1–25, 2021.

[43] F. Trotta, M. Zanetti, and G. Camino, "Thermal degradation of cyclodextrins," *Polym. Degrad. Stab.*, vol. 69, pp. 373–379, 2000.

[44] N. K. Dhakar *et al.*, "Evaluation of solubility enhancement, antioxidant activity, and cytotoxicity studies of kynurenic acid loaded cyclodextrin nanosponge," *Carbohydr. Polym.*, vol. 224, pp. 1–9, 2019.

[45] I. Krabicová *et al.*, "History of cyclodextrin nanosponges," *Polymers (Basel).*, vol. 12, no. 5, pp. 1–23, 2020.

[46] G. Hoti *et al.*, "Nutraceutical Concepts and Dextrin-Based Delivery Systems," *Int. J. Mol. Sci.*, vol. 23, no. 8, pp. 1–47, 2022.

[47] M. Petitjean, I. X. García-Zubiri, and J. R. Isasi, "History of cyclodextrin-based polymers in food and pharmacy: a review," *Environ. Chem. Lett.*, pp. 1–12, 2021.

[48] J. Hukkanen, O. Pelkonen, and H. Raunio, "Expression of xenobiotic-metabolizing enzymes in human pulmonary tissue: possible role in susceptibility for ILD," *Eur Respir J*, vol. 18, no. 32, pp. 122–126, 2001.

[49] B. Evrard *et al.*, "Cyclodextrins as a potential carrier in drug nebulization," *J. Control. Release*, vol. 96, no. 3, pp. 403–410, 2004.

[50] V. Vartiainen, L. M. Bimbo, J. Hirvonen, E. I. Kauppinen, and J. Raula, "Aerosolization, Drug Permeation and Cellular Interaction of Dry Powder Pulmonary Formulations of Corticosteroids with Hydroxypropyl-β-Cyclodextrin as a Solubilizer," *Pharm. Res.*, vol. 34, no. 1, pp. 25–35, 2017.

[51] G. Salzano *et al.*, "Cyclodextrin-based nanocarriers containing a synergic drug combination: A potential

formulation for pulmonary administration of antitubercular drugs," *Int. J. Pharm.*, vol. 531, no. 2, pp. 577–587, 2017.

[52] L. Matilainen *et al.*, "In vitro toxicity and permeation of cyclodextrins in Calu-3 cells," *J. Control. Release*, vol. 126, pp. 10–16, 2008.

[53] J. Costa-Gouveia *et al.*, "Combination therapy for tuberculosis treatment: pulmonary administration of ethionamide and booster co-loaded nanoparticles," *Sci. Rep.*, vol. 7, no. 5390, pp. 1–14, 2017.

[54] P. K. Shende, F. Trotta, R. S. Gaud, K. Deshmukh, R. Cavalli, and M. Biasizzo, "Influence of different techniques on formulation and comparative characterization of inclusion complexes of ASA with β-cyclodextrin and inclusion complexes of ASA with PMDA cross-linked β-cyclodextrin nanosponges," *J Incl Phenom Macrocycl Chem*, vol. 74, pp. 447–454, 2012.

[55] P. Shende *et al.*, "Acute and Repeated Dose Toxicity Studies of Different β-Cyclodextrin-Based Nanosponge Formulations," *J. Pharm. Sci.*, vol. 104, pp. 1856–1863, 2015.

[56] S. H. Shahiwala, A.F., Sammour, R.M., Almurisi and M. Taher, "Proniosomes For Oral Delivery Of Aceclofenac: Impact Of Paddle Versus Dialysis Methods On In Vitro-In Vivo Correlation (Ivivc) Predictions.," *Drug Deliv. Lett.*, 2023.

[57] M. Havrdova *et al.*, "Toxicity of carbon dots-Effect of surface functionalization on the cell viability, reactive oxygen species generation and cell cycle," *Carbon N. Y.*, vol. 99, pp. 238–248, 2016.

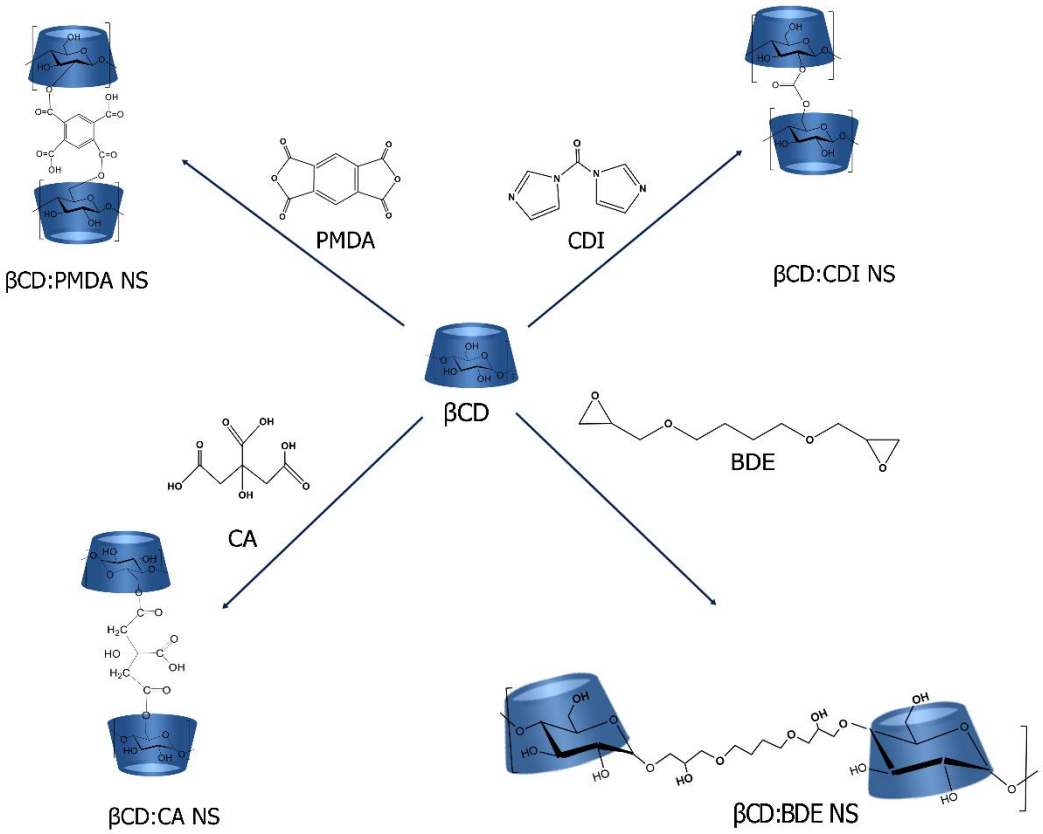

Figure 1. Schematic representation of βCD-based nanosponges (*βCD: CDI NS*; *βCD: PMDA NS; βCD: CA NS; and βCD: BDE NS).*

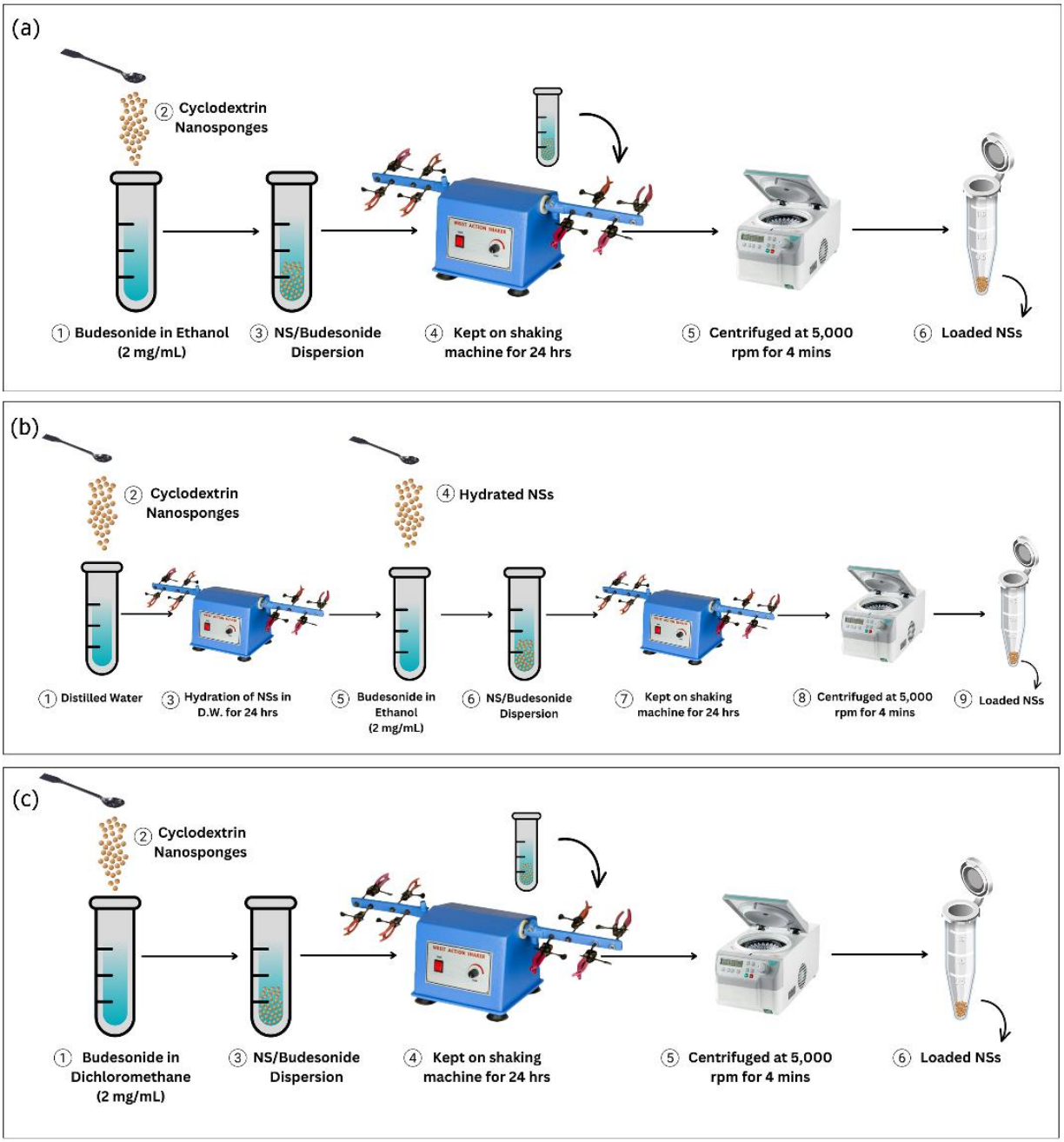

Figure 2. Schematic illustration of BUD-loaded NS using three different loading methods (labelled as method A, B, and C).

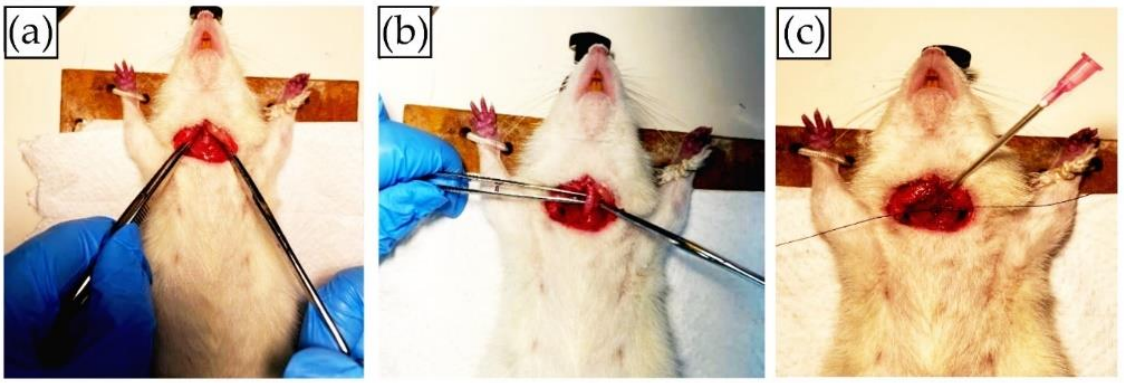

672

673 **Figure 3.** (a) Incision in front of throat; (b) removal of tissue in front of trachea; (c) insertion of the tube into the trachea.

674

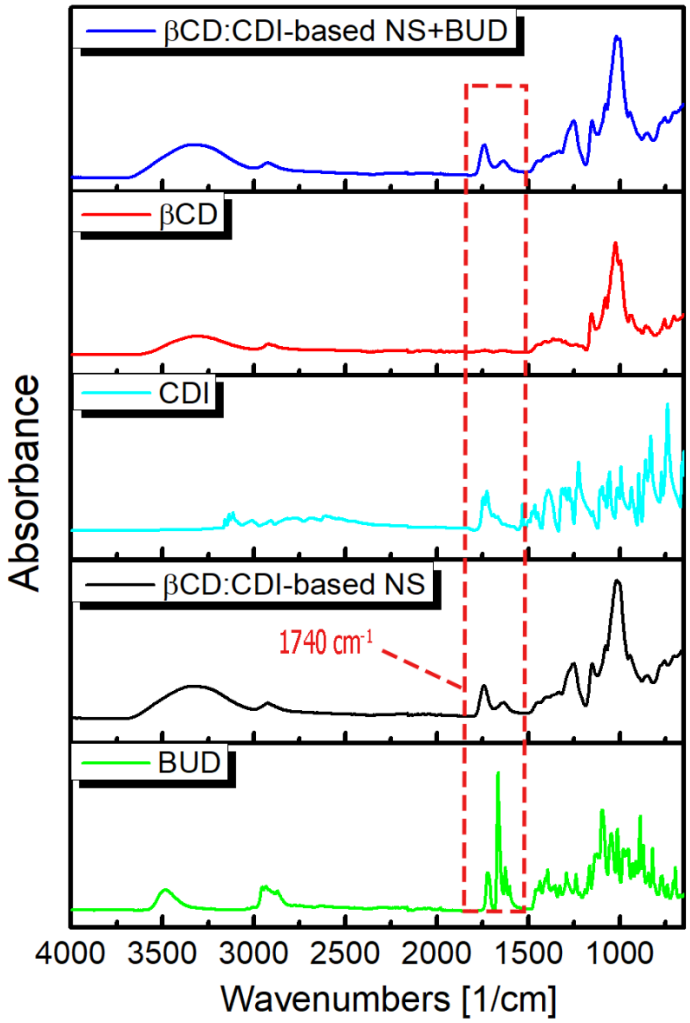

675

676 **Figure 4.** FTIR spectra of pure BUD, blank βCD: CDI-based NS, and BUD-loaded βCD: CDI-based NS.

677

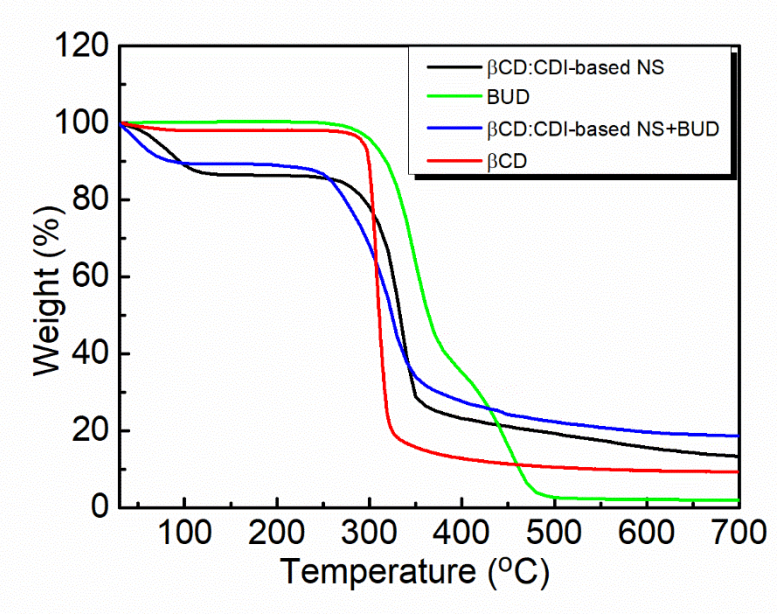

Figure 5. Thermogravimetric analysis (TGA) of pure BUD, βCD, blank βCD-NS, and BUD-βCD-NS.

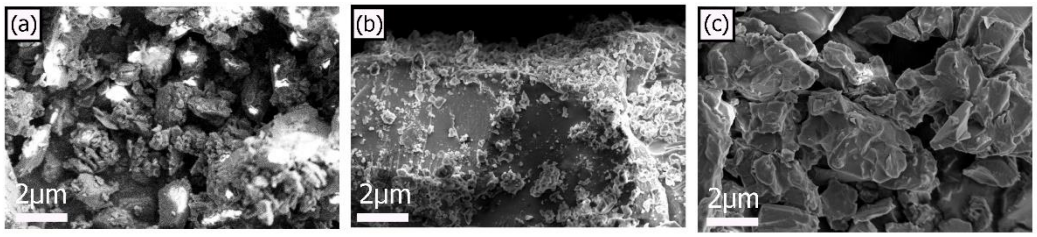

Figure 6. SEM images of a) BUD; b) βCD-NS+ BUD physical mixture; c) BUD-βCD-NS.

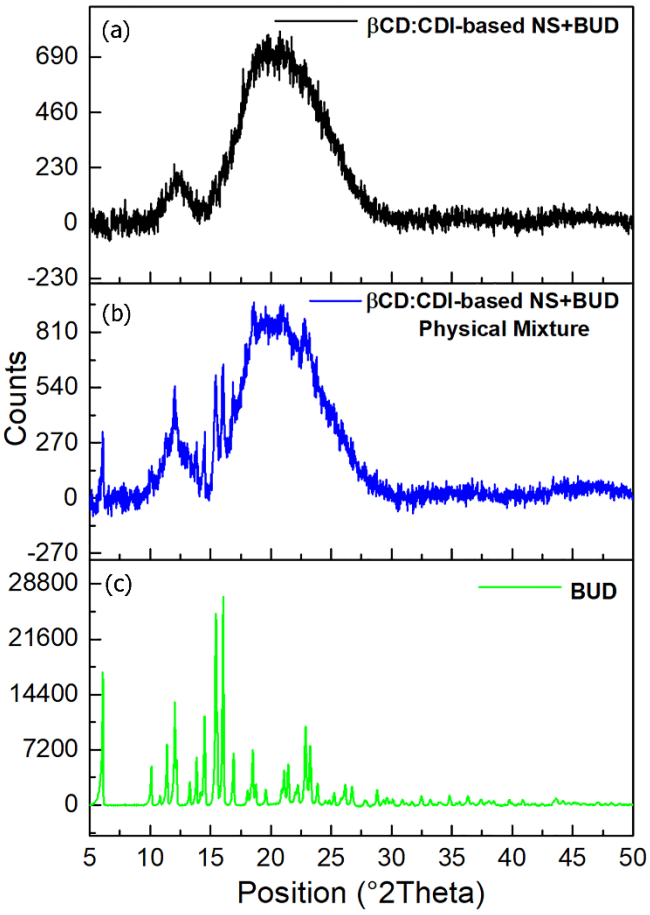

Figure 7. XRD analysis of a) BUD-βCD-NS; b) βCD-NS+ BUD physical mixture; and c) Budesonide (BUD).

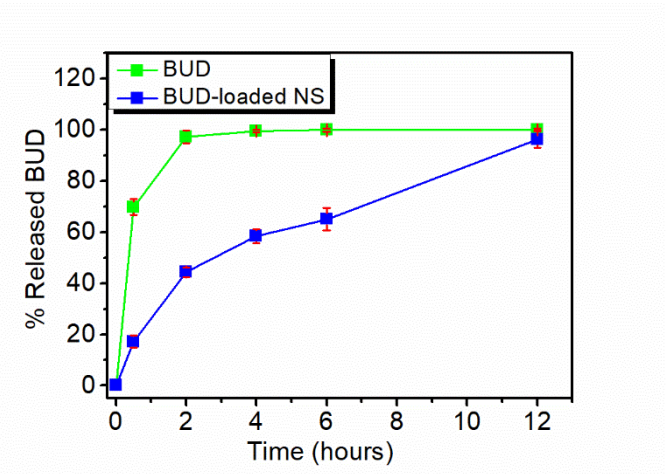

Figure 8. In vitro drug release profile of BUD-βCD-NS and pure BUD in phosphate buffer saline solution (PBS) pH 7.4.

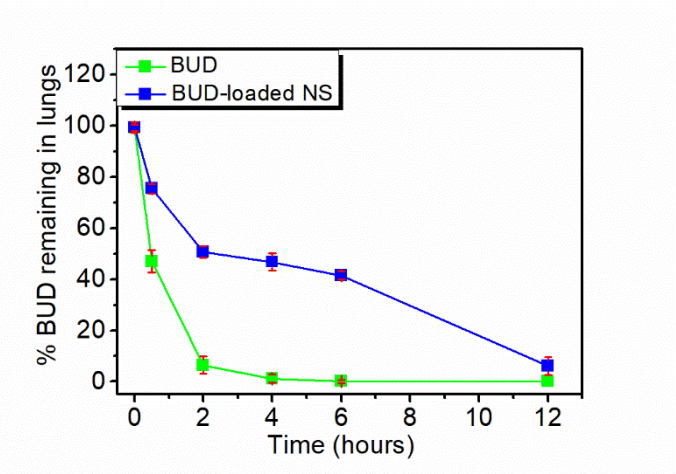

Figure 9. In vivo study of BUD-βCD-NS and Pure BUD.

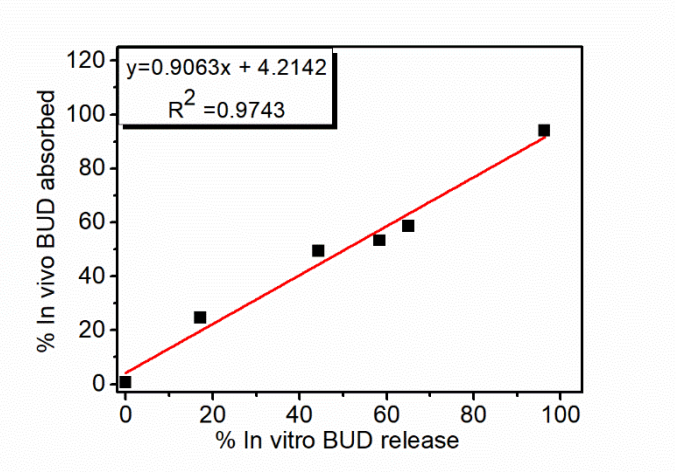

Figure 10. Linear correlations between the % release in vitro and % absorbed in vivo for F3.

721 **Table 1.** Budesonide Loaded Nanosponges Formulations.

722

Formula Code	BUD:NS (w:w)	NS
F1	1:1	βCD:CDI
F2	1:2	
F3	1:3	
F4	1:4	
F5	1:1	βCD:PMDA
F6	1:2	
F7	1:3	
F8	1:4	
F9	1:1	βCD:CA
F10	1:2	
F11	1:3	
F12	1:4	
F13	1:1	βCD:BDE
F14	1:2	
F15	1:3	
F16	1:4	
F17	1:1	LC:CA
F18	1:2	
F19	1:3	
F20	1:4	

723
724
725
726
727 **Table 2.** Encapsulation efficiency (EE%) and Loading capacity (LC%) of BUD loaded NS.

Formulations	NS type	BUD:β CD-NS	Encapsulation Efficiency %			Loading Capacity %		
			Method A	Method B	Method C	Method A	Method B	Method C
F1	βCD: CDI	1:1	2.10	11.59	72.50	2.1	11.59	72.50
F2		1:2	3.50	12.80	74.60	1.75	6.40	37.30
F3		**1:3**	**6.30**	17.45	**81.00**	2.1	5.81	27.00
F4		1:4	4.90	9.54	67.36	1.22	2.39	16.84
F5	βCD: PMDA	1:1	--	2.40	24.23	--	2.40	24.23
F6		1:2	--	3.20	26.60	--	1.60	13.30

F7		1:3	--	5.66	29.80	--	1.88	9.93
F8		1:4	--	10.70	30.40	--	2.67	7.60
F9		1:1	--	--	18.89	--	--	18.89
F10	βCD:CA	1:2	--	1.18	21.40	--	0.59	10.70
F11		1:3	--	4.78	25.00	--	1.59	8.33
F12		1:4	--	5.80	22.60	--	1.45	5.65
F13		1:1	--	8.24	49.90	--	8.24	49.90
F14	βCD:BDE	1:2	0.89	9.70	57.60	0.44	4.85	28.80
F15		1:3	2.40	13.86	62.70	0.80	4.62	20.90
F16		1:4	--	15.00	65.00	--	3.75	16.25
F17		1:1	--	2.80	32.80	--	2.80	32.80
F18	LC:CA	1:2	--	6.90	39.13	--	3.45	19.56
F19		1:3	--	8.94	43.50	--	2.98	14.50
F20		1:4	--	16.80	52.80	--	4.20	13.20

Table 3. Water absorption capacity (WAC) experimental values of the synthesized nanosponges (NS).

Nanosponges (NS)	WAC (%)
βCD:CDI	**179 ± 22**
βCD:PMDA	532 ± 18
βCD:CA	317 ± 21
LC:CA	292 ± 7
βCD:BDE	458 ± 13

Table 4. Particle size, zeta potential, and PDI for F3 and blank NS.

βCD-CDI NS	Particle size	PDI	Zeta potential
Blank	106.96 ± 15.04 nm	1.30%	5.2 ± 1.6 mV
F3	406.90 ± 10.70 nm	26.90%	-2.6 ± 0.6 mV

Table 5. In vitro drug release study.

Formula	Time (hours)	% Released Drug
Pure BUD	0	0
	0.5	69.77±3.08
	2	97.27±2.59
	4	99.53±0.54
	6	99.91±0.59
	12	100±0.29
F3	0	0
	0.5	17.23±2.43
	2	44.35±1.92
	4	58.47±2.71
	6	65.06±4.39
	12	96.33±3.23

Table 6. % BUD remaining in lungs during the in vivo study.

Formula	Time (hours)	% drug remaining
Pure BUD	0	99.25±1.20
	0.5	46.96±4.32
	2	6.40±3.39
	4	1.19±1.59
	6	-0.15±0.63
	12	-
F3	0	99.35±2.10
	0.5	75.36±1.94
	2	50.64±2.26
	4	46.77±3.49
	6	41.44±1.61
	12	6.10±3.46

769 **Table 7**. Aerosol performance of BUD-βCD-NS.
770

Properties of BUD-NS	Mean±SD
Angle of repose	26.17±2.10
Compressibility Index	9.10±0.30
Hausner ratio	1.11±0.04
FPF (%)	45.14±3.60
ED (%)	92.40±0.84
MMAD	4.17±0.30
GSD	2.10±0.20

771